Mineralogy and Petrology (1998) 62: 223–245

Mineralogy and Petrology

Mildly alkaline basalts from Pavagadh Hill, India: Deccan flood basalts with an asthenospheric origin

J. D. Greenough[1], **K. R. Hari**[2], **A. C. Chatterjee**[3], and **M. Santosh**[4]

[1] Department of Earth and Ocean Sciences, University of British Columbia, Okanagan University College, Kelowna, B.C., Canada
[2] Department of Geology, Government Arts and Science College, Durg (M.P.), India
[3] School of Studies in Geology, Vikram University, Ujjain (M.P.), India
[4] Centre for Earth Science Studies, Akkulam, Trivandrum, India

With 6 Figures

Received April 15, 1996;
revised version accepted July 25, 1997

Summary

Of twelve flows at Pavagadh Hill, the two three-phenocryst-basalt flows with Mg#~0.70 and Ni/MgO~33 are the most primitive and perhaps as primitive as any basalts in the Deccan province. Scatter on variation diagrams and the occurrence of primitive flows at two different levels in the volcanic sequence implies that most rocks are probably not, strictly speaking, comagmatic. Nevertheless, mass balance calculations indicate a generalized differentiation scheme from primitive basalt to hawaiite that involved removal of olivine, augite, plagioclase and Fe-Ti oxides in the proportions 40:33:22:5 with ~ 50% of the magma remaining. Crustal assimilation had a minimal effect on evolution of the basalts but rhyolites at the top of the volcanic sequence may have been produced by crustal melting following prolonged heat release from alkali basalt pooled along fault zones in the continental crust. Major element based calculations indicate that the most primitive basalts were generated by 7 to 10% melting of mantle peridotite. These low percentages of melting, typical of alkali basalts, are consistent with the steep slopes on chondrite-normalized REE diagrams. Low heavy REE concentrations point to residual garnet in the source region. Incompatible element concentrations (e.g. Rb, Ba, Zr, La) in Pavagadh basalts exceed those in Deccan tholeiitic basalts but are substantially lower than those reported for some other Deccan alkali basalts. Obviously Pavagadh basalts do not reflect the lowest percentages of melting and greatest amount of source region metasomatic enrichment attained in the Deccan province. Deccan tholeiitic and alkali basalts are largely characterized by low La/Nb ratios and high La/Ba ratios similar to those in oceanic island basalts. This

indicates minimal involvement of the subcontinental lithospheric mantle in their petrogenesis. Comparison with continental mafic magma provinces where a subcontinental lithospheric mantle imprint is common indicates long periods of extension and/or melting of mantle lithosphere still hot from pre-extension subduction are more likely to produce magmas bearing the lithospheric imprint.

Zusammenfassung

Alkalische Basalte von Pavagadh Hill, Indien: Deccan-Flutbasalte von Asthenosphärischer Herkunft

Im Gebiet von Pavagadh Hill, Indien, treten 12 Spät-Deccan und rhyolithische alkalibasaltische Ergüsse und Intrusiva auf. Variationsdiagramme zeigen, daß die Abfolge nicht komagmatisch ist. Zusammen mit Berechnungen der Massenbilanz unterstützen sie vielmehr ein Zwei-Stadienmodell für die Entstehung von Hawaiiten aus sehr primitiven (i.e. $Mg\# = Mg/(Mg+.(0.9*Fe_{total}))$ at.%~0.70) Basalten. Olivin und Augit dominierten die frühe Fraktionierung während Augit vorherrschte als der Magmaanteil von 65% auf 50% sank. Die Entfernung von Plagioklas spielte bei der Differentiation nur eine geringe Rolle. Niedrige Th/Nb (~0,2), Rb/Sr(<0,12) und K/Nb-Verhältnisse geben keine Hinweise auf signifikante Assimilation von Krustenmaterial. Die Seltene-Erd-Verteilungsmuster (SEE), niedrige Gehalte an schweren SEE sowie die Hauptelementspektren der Alkalibasalte weisen auf eine granatführende Ursprungsregion und auf einen Aufschmelzungsgrad von nur 7% bis 10% hin. Es gibt jedoch auch stärker alkalische (höhere Rb, Zr etc.) Deccanbasalte (i.e. Rajpipla). Die Assoziation von Deccanalkalibasalten, Rhyolithen und Störungszonen zeigt, daß letztere die Extraktion von Magma aus dem Mantel erleichterten und dazu führten, daß Magma aus Magmenkammern Krustenschmelzen (Rhyolithe) produzierte. Deccanbasalte tendieren zu hohen La/Ba und niedrigen La/Nb-Verhältnissen; dies weist auf eine asthenosphärische Herkunft hin, selbst wenn die Gesteine verhältnismäßig spät gebildet wurden (i.e. Pavagadh). Längere Perioden von Krustenextension oder von Subduktion, die der Extension vorhergeht, führt offensichtlich zur Entstehung von Magmen mit einer lithosphärischen Komponente.

Introduction

The Deccan Traps of India cover one fifth of the total Indian sub-continent. Most basalts formed during a tumultuous Tertiary event that possibly lasted $\leq$0.5 m.y. (*White*, 1989). The abbreviated time span and dominance of tholeiitic basalts are features shared with other flood basalt povinces (Ibid.). Alkali basalts and various "differentiated" rocks also occur (*Krishnamurthy* and *Cox*, 1980) but form a small portion of Deccan stratigraphy. Studies of Cenozoic continental mafic rocks in the Western United States show that alkaline magmas are important for establishing models to explain temporal and spatial changes in basalt chemistry. They are also important for investigating the role of plume versus subcontinental lithospheric mantle in the generation of basalts because in many cases the alkaline volcanism occurs early and/or late in the volcanic episode (*Fitton* et al., 1988, 1991; *Basu* et al., 1993) thus monitoring lithospheric involvement with time.

Extrusive igneous rocks ranging from alkali olivine basalts to rhyolites occur over an area of 35 km^2 at Pavagadh Hill near Gujarat, India (Fig. 1). They represent

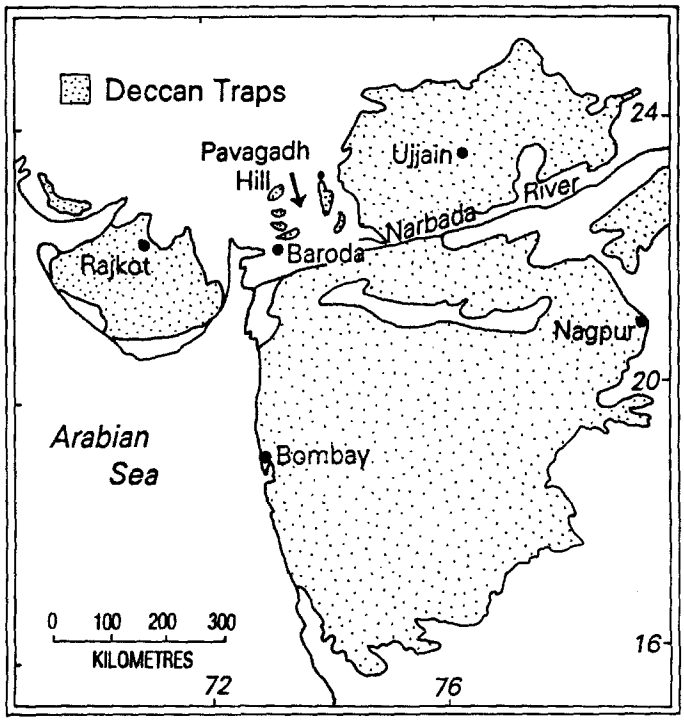

Fig. 1. Map of the Deccan Traps showing the location of Pavagadh Hill

late (63.5±2 Ma) Deccan volcanism (*Alexander*, 1981) and have been controversial. *Chatterjee* (1961) regarded them as an outlier of the Deccan Traps and suggested that differentiation of alkali basalt produced all rock types in the area with the exception of rhyolites. However, *Sinha* and *Tiwari* (1964) and *Tiwari* (1971) opined that olivine basalt and all its alkaline derivatives were related to silica oversaturated basalts in the area. *Alexander* (1980) suggested that the rhyolites formed through crustal contamination of basalt. *Hari* et al. (1991) proposed an alkali basalt parent magma for mafic rocks in the area based on a study of melt inclusions in olivine phenocrysts.

In this study we present a comprehensive set of major and trace element data for the Pavagadh Hill basalts. These data are used to constrain basalt petrogenesis and investigate involvement of asthenospheric mantle, lithospheric mantle and continental crust in the origin of alkaline flood basalts.

Field relations and age

The Pavagadh igneous complex overlies middle Cretaceous sandstones belonging to the Bagh Formation. Underlying the sandstones are middle Proterozoic phyllite, slate, quartzite and meta-conglomerate of the Champaner Group (*Krishnan*, 1982). Most exposures of igneous rocks occur at Pavagadh Hill. Detailed mapping resolved previous differences of opinion as to the total number of lava flows. We recognize 12 units, mostly lava flows, with lithologies and thicknesses given in

Table 1. *Pavagadh Hill stratigraphy*

Flow No.	Rock types	thickness (m)
12	Rhyolite	?
11	Rhyodacite, Ignimbrite, Pitchstone	120
10	Hawaiite	75
9	Hawaiite	60
8	Basalt	25
7	Hawaiite (locally inter-layered with mugearite)	40
6	Three-phenocryst basalt	35
5	Hawaiite	40
4	Basalt	35
3	Ankaramite	40
2	Three-phenocryst basalt	30
1	Olivine basalt	115

Table 1. In addition mugearite occurs as dykes and sub-horizontal lenses that disappear above flow no. 7. Contrary to previous suggestions, mugearite flows were not observed. Details of the distribution and field appearance of the rocks are given in *Hari* (1991). *Alexander* (1981) reports a K-Ar age of 63.5 Ma for basalts from the Pavagadh sequence that is consistent with previously reported ages for various rock types in the sequence.

Petrography

Based on petrography, 8 rock types are recognizable at Pavagadh Hill: olivine basalt, three-phenocryst basalt, ankaramite, basalt, hawaiite, mugearite, rhyolite and rhyodacite. Summary rock descriptions appear below with details in *Hari* (1991). Representative electron microprobe analyses of phases in flow no. 1 appear in Table 2.

The *olivine basalt* contains olivine (26%) and augite phenocrysts (11%), the former as macrophenocrysts ~5 mm long (Fo_{86-75}) and microphenocrysts ~1.6 mm long (Fo_{86-66}). The groundmass consists of plagioclase, augite and olivine with accessory titanomagnetite, apatite and glass. The *three-phenocryst basalt* contains zoned plagioclase (An_{64-60}), augite and partially resorbed olivine phenocrysts. Plagioclase (An_{60-58}) and augite comprise the groundmass together with accessory biotite, titanomagnetite, chalcopyrite and sporadic calcite. The *ankaramite* has augite (dominant) and olivine phenocrysts with groundmass plagioclase, augite and minor biotite, titanomagnetite, ilmenite, and glass. *Basalt* samples lack olivine. Plagioclase (An_{64-62}) and augite phenocrysts sit in a groundmass bearing the same minerals plus accessory titanomagnetite, ilmenite and glass. The above rocks show minor alteration with hematite, chlorophaeite, iddingsite and serpentine locally apparent.

Table 2. *Olivine basalt mineral analyses*

Olivine analysis					*Clino-pyroxene analysis*				
	Grain-1		*Grain-2*			*Grain-1*		*Grain-2*	
Oxide	Core	Rim	Core	Rim	Oxide	Core	Rim	Core	Rim
SiO_2	40.21	38.03	40.45	35.34	SiO_2	52.66	53.02	52.12	50.95
TiO_2	0.00	0.00	0.00	0.00	TiO_2	0.22	0.57	0.49	0.54
Al_2O_3	0.00	0.00	0.00	0.00	Al_2O_3	2.45	3.02	1.50	0.00
FeO*	13.12	23.57	13.82	28.84	FeO*	6.16	5.65	7.23	11.10
MnO	0.65	1.09	0.50	1.25	MnO	0.00	0.56	0.52	0.66
MgO	43.46	39.08	45.59	32.07	MgO	15.55	15.75	16.28	13.37
CaO	0.63	0.39	0.44	0.00	CaO	22.35	22.28	20.46	21.27
SUM	98.07	102.16	100.80	97.51	SUM	99.39	100.85	98.60	97.89
O =	4.00	4.00	4.00	4.00		6.00	6.00	6.00	6.00
Si	0.994	0.979	1.001	0.996		1.947	1.931	1.956	1.969
Ti	–	–	–	–		0.006	0.016	0.014	0.016
Al	–	–	–	–		0.107	0.129	0.067	–
Fe	0.271	0.507	0.286	0.662		0.190	0.172	0.227	0.359
Mn	0.013	0.024	0.007	0.029		–	0.017	0.017	0.021
Mg	1.711	1.500	1.682	1.313		0.857	0.855	0.908	0.770
Ca	0.017	0.011	0.011	–		0.855	0.869	0.820	0.880
SUM	3.006	3.021	2.987	3.000	SUM	3.992	3.989	4.009	4.015
Mole %					Wo	46.00	46.00	46.00	44.00
Fo	86.30	74.10	85.50	66.50	En	44.00	45.00	46.40	38.00
					Fs	10.00	9.00	11.60	18.00

Grain-1: Macro phenocryst, Grain-2: Micro phenocryst.
Note: Analysis in wt%. * Total Fe as Feo

Plagioclase (An_{32}) and augite phenocrysts in *hawaiite* sit in a plagioclase and augite trachytic groundmass with accessory olivine, titanomagnetite, ilmenite, and glass. *Mugearite* contains various xenocryst phases reflecting the rock type intruded locally. The groundmass exhibits a trachytic to sub-trachytic texture dominated by plagioclase and lesser amounts of augite, titano-magnetite, ilmenite, secondary hematite and glass. The *rhyolite* is characterized by a fine-grained quartzo-feldspathic groundmass bearing quartz and potassium feldspar phenocrysts and glass. The *rhyodacite* and associated pitchstone and ignimbrite contain phenocrysts of plagioclase and minor augite, fayalitic olivine and quartz in a quartzo-feldspathic groundmass containing glass. Alteration is not readily apparent in the leucocratic rocks but celadonite spherulites and the local replacement of plagioclase by calcite is apparent in the hawaiites.

Geochemistry

Analytical methods

Nineteen representative samples were analyzed for their major elements by AAS. Due to partial oxidation in most rocks, total iron is reported as Fe_2O_3. Loss on ignition was determined by heating to 1050 °C. Zr, Nb, Ga, V, Cu, Zn, Sc, Ni and Cr were determined by X-Ray fluorescence methods. Precision and accuracy as estimated from replicate analyses of international standards is ±5% for all elements except Cu (±10%). The remaining 33 trace elements were analyzed by inductively coupled plasma-mass spectrometry following *Longerich* et al. (1990) with precision and accuracy better than 4%. All analytical work was performed at The Memorial University of Newfoundland, Canada.

Presentation of data

Major and trace element data (Table 3) plotted against the differentiation indicator Mg# ($Mg\# = Mg/(Mg \pm 0.9Fe_{total})$ atomic) exhibit clear differentiation trends (Fig. 2). However, basalt samples (ankaramites, basalt, olivine basalt and three-phenocryst basalts) show some scatter (e.g. Mg# versus Al_2O_3, Nb, La) and mugearites tend to plot furthest from the overall trend lines (e.g. Al_2O_3, Sr, La, Yb and Y; Fig. 2). Aluminum increases with decreasing Mg# in the basalts, peaks in the hawaiites, and then decreases with higher Mg# whereas CaO peaks in the basalts. Three-phenocryst basalts (GP252 and GP229) have very high Mg# values (≤ 0.72), high Ni and Cr (≤ 474 ppm and ≤ 844 ppm; Fig. 2) and the lowest incompatible element concentrations (e.g. Zr, Rb, Sr) in the suite.

A plot of Zr (ppm) against TiO_2 (oxide wt.%, Fig. 3) and Nb/Y ratios > 1 (mean of 8 most MgO-rich samples $= 1.9$, $\sigma = 1.0$) attest to the mildly alkaline tendencies of the Pavagadh Hill basalts. Chondrite-normalized rare earth element (REE) patterns (Fig. 4) are near-parallel with moderate to steep slopes typical of alkali basalts. Normalized Yb and Lu are around 6 in samples with high MgO contents. Oceanic island basalt-normalized diagrams lack positive Ba anomalies and negative Ti and Nb anomalies (Fig. 5).

Table 3. *Whole rock analyses of Pavagadh rocks*

	GP229	GP252	GP255	GP277	GP240	GP216	GP61	GP221	GP224	GP219
SiO_2	45.40	45.80	46.40	42.90	50.40	47.90	48.00	46.70	49.30	48.40
TiO_2	1.80	2.00	1.64	1.92	1.72	1.96	1.64	2.04	2.24	2.12
Al_2O_3	11.00	11.30	12.10	10.10	11.90	12.70	12.90	15.40	15.50	15.50
Fe_2O_3	11.89	12.71	12.08	11.32	11.11	12.47	10.98	12.78	12.41	12.71
MnO	0.17	0.16	0.17	0.16	0.15	0.18	0.14	0.17	0.18	0.18
MgO	13.70	12.58	11.55	9.41	8.22	7.30	5.87	4.92	4.08	4.11
CaO	9.56	9.64	9.92	11.10	10.80	11.16	11.38	10.16	7.96	9.18
Na_2O	1.65	1.82	1.75	1.37	2.11	2.12	1.75	2.44	2.93	2.96
K_2O	0.67	0.77	0.82	1.05	1.21	0.88	1.31	1.24	2.53	1.42
P_2O_5	0.21	0.25	0.18	0.27	0.22	0.23	0.32	0.28	0.35	0.36
LOI	3.08	2.16	2.76	10.04	1.51	1.85	6.07	2.25	2.05	2.81
Total	99.13	99.19	99.37	99.64	99.35	98.75	100.36	98.38	99.53	99.75
Mg#	0.72	0.69	0.68	0.65	0.62	0.56	0.54	0.50	0.42	0.42
Large Ion Lithophile Elements										
Li	5.85	6.60	1.51	9.43	5.27	7.34	3.73	4.90	11.7	10.5
Rb	18.4	12.0	1.27	17.8	39.2	15.4	28.6	31.0	66.7	38.1
Cs	0.88	0.32	0.022	0.39	0.30	0.068	0.47	0.22	0.61	0.30
Sr	291	275	185	300	310	392	969	450	427	497
Ba	169	182	179	290	312	287	472	375	590	449
Be	0.82	0.87	0.88	0.99	1.10	1.28	1.06	0.86	1.35	1.28
High Field Strength Elements										
Th	2.57	2.26	0.60	4.72	6.00	5.16	5.98	4.61	7.16	7.38
U	0.65	0.62	0.53	0.61	1.23	1.26	1.19	0.97	1.52	1.52
Zr	142	164	128	159	162	170	181	164	231	223
Hf	3.69	3.52	2.82	3.52	4.33	4.39	4.20	4.64	4.76	5.60
Nb	24	29	23	37	24	29	26	30	35	33
Ta	1.75	1.46	1.40	0.47	1.80	1.92	1.71	3.04	0.64	2.34
Y	16.6	16.2	5.11	17.6	19.0	21.0	22.0	18.7	24.3	25.5
Rare Earth Elements										
La	18.5	19.1	9.26	29.7	27.8	27.5	30.0	28.1	38.2	40.0
Ce	40.8	42.3	21.2	59.7	57.6	58.4	59.6	59.1	76.8	88.9
Pr	5.16	5.20	2.62	7.06	6.81	7.10	7.08	7.16	9.02	9.63
Nd	20.8	21.4	10.8	26.2	26.6	23.4	27.3	28.1	34.4	36.8
Sm	4.64	4.62	2.24	5.25	5.51	5.84	5.71	5.78	6.85	7.35
Eu	1.53	1.36	0.64	1.47	1.62	1.76	3.73	1.91	1.95	2.20
Gd	4.34	3.98	1.79	3.89	5.52	5.17	5.64	5.36	6.06	6.55
Tb	0.65	0.62	0.28	0.64	0.78	0.78	0.78	0.76	0.88	0.98
Dy	3.72	3.64	1.61	3.63	4.42	4.63	4.44	4.44	5.31	5.56
Ho	0.69	0.66	0.29	0.68	0.83	0.83	0.84	0.86	1.01	1.06
Er	1.94	1.92	0.88	1.93	2.34	2.37	2.38	2.41	2.85	3.07
Tm	0.25	0.24	0.11	0.25	0.31	0.31	0.32	0.31	0.39	0.41
Yb	1.56	1.37	0.64	1.52	1.84	1.96	2.02	2.09	2.39	2.53
Lu	0.22	0.20	0.082	0.21	0.28	0.29	0.28	0.30	0.35	0.37
Sc	23	27	30	35	31	30	31	23	24	21
V	278	309	274	138	245	336	248	298	361	336
Cr	844	657	557	454	325	137	261	n.d.	n.d.	n.d.

(*continued*)

Table 3 *(continued)*

	GP229	GP252	GP255	GP277	GP240	GP216	GP61	GP221	GP224	GP219
Ni	474	405	205	234	150	131	125	21.00	n.d.	n.d.
Mo	2.5	1.9	2.1	0.60	1.6	1.5	1.5	1.2	1.1	1.5
Cu	129	115	31	104	120	113	112	53	26	216
Zn	63	69	58	67	63	69	77	58	81	67
Pb	2.98	3.36	3.31	4.30	6.15	4.34	7.12	4.66	7.39	6.69
Bi	0.015	0.018	0.018	0.027	0.039	0.019	0.046	0.005	0.012	0.016
Tl	0.008	0.025	0.011	0.041	0.068	0.023	0.131	0.059	0.214	0.061
Ga	16	19	17	13	19	18	18	19	24	23

	GP220	GP222	GP285	GP225	GP239	GP210	GP214	GP235	GP291
SiO_2	47.70	48.30	47.60	54.80	54.70	67.00	73.10	67.20	74.80
TiO_2	2.28	2.48	2.48	2.16	2.12	0.60	0.44	0.72	0.28
Al_2O_3	15.60	15.10	14.30	13.60	13.50	14.00	12.90	13.60	12.20
Fe_2O_3	12.39	13.33	14.73	11.89	11.96	5.02	2.71	5.25	3.17
MnO	0.18	0.14	0.20	0.15	0.15	0.11	0.12	0.12	0.08
MgO	3.98	3.74	4.74	3.00	2.82	0.33	0.12	0.54	0.06
CaO	9.26	8.56	9.36	7.50	7.14	1.66	0.70	2.18	0.24
Na_2O	3.03	3.21	2.84	2.72	2.76	3.44	3.85	4.86	3.60
K_2O	1.48	1.78	1.39	1.27	1.34	5.44	5.20	3.18	5.05
P_2O_5	0.38	0.41	0.42	0.39	0.43	0.07	0.02	0.11	0.00
LOI	2.51	1.98	1.92	1.55	1.86	1.48	0.81	2.25	0.88
Total	98.79	98.98	99.71	99.03	99.78	99.15	99.91	100.04	100.36
Mg#	0.41	0.38	0.40	0.36	0.34	0.13	0.09	0.18	0.04
Large Ion Lithophile Elements									
Li	10.5	8.37	1.65	3.75	11.7	19.0	22.4	14.2	17.7
Rb	37.2	66.2	7.59	8.23	22.9	195	202	184	172
Cs	0.31	0.66	0.02	0.008	0.089	2.2	2.9	3.4	2.8
Sr	483	466	225	169	393	180	118	194	63.6
Ba	460	512	152	247	444	929	923	915	910
Be	1.52	1.47	1.50	1.42	1.39	3.86	4.21	4.86	4.08
High Field Strength Element									
Th	7.45	8.35	0.984	1.62	6.95	30.2	30.7	30.3	28.0
U	1.59	1.73	1.04	1.25	1.33	5.19	7.61	7.06	5.51
Zr	230	258	245	253	269	536	653	567	575
Hf	5.74	6.19	6.00	5.67	5.80	13.5	12.9	15.0	8.29
Nb	34	39	54	40	41	62	80	67	82
Ta	2.37	2.60	3.33	2.56	0.71	4.07	3.52	4.14	4.28
Y	25.2	27.5	5.94	10.7	40.2	50.4	45.8	53.3	68.8
Rare Earth Elements									
La	41.1	43.8	17.2	18.2	45.5	94.3	93.0	91.7	64.3
Ce	84.6	88.8	41.2	43.0	86.2	178	193	181	120
Pr	9.92	10.5	4.31	4.56	10.9	20.8	21.4	21.1	15.9
Nd	37.2	39.8	16.8	17.9	42.3	73.2	78.1	75.0	57.0
Sm	7.59	8.00	3.29	3.66	8.91	13.9	15.2	14.6	11.4

(continued)

Table 3 *(continued)*

	GP220	GP222	GP285	GP225	GP239	GP210	GP214	GP235	GP291
Eu	2.26	2.35	0.93	0.97	2.55	3.22	3.17	3.05	2.33
Gd	6.91	7.38	2.45	3.09	8.13	11.9	13.1	12.2	10.5
Tb	1.01	1.08	0.36	0.48	1.26	1.85	2.06	1.94	2.13
Dy	5.79	6.24	1.99	2.69	7.45	10.6	11.5	11.4	14.3
Ho	1.08	1.19	0.36	0.50	1.45	2.04	2.10	2.18	2.90
Er	3.20	3.24	0.94	1.46	1.13	5.87	5.94	6.57	8.54
Tm	0.41	0.44	0.12	0.19	0.53	0.81	0.83	0.93	1.15
Yb	2.56	2.71	0.74	1.06	3.37	5.24	5.18	5.97	6.84
Lu	0.38	0.37	0.10	0.16	0.48	0.76	0.75	0.88	0.96
Sc	22	27	32	22	23	9	6	7	3
V	344	336	417	267	271	5	n.d.	2	3
Cr	n.d.	n.d.	n.d.	59	23	184	5	65	1
Ni	n.d.	n.d.	10	51	36	60	n.d.	21	n.d.
Mo	2.0	1.9	2.1	4.9	1.5	14.6	4.7	6.2	2.7
Cu	17	16	77	160	169	14	11	9	23
Zn	71	82	102	94	95	85	85	89	96
Pb	6.58	6.94	19.1	3.68	5.47	21.5	23.3	23.6	25.4
Bi	0.016	0.026	0.028	0.006	0.007	0.27	0.086	0.13	0.054
Tl	0.60	0.16	0.036	0.040	0.046	0.60	0.65	0.80	0.50
Ga	23	23	23	21	20	23	22	22	22

Major element analyses in wt.% with total Fe as Fe_2O_3. LOI = loss on ignition. Trace element concenrations in ppm. Mg# = (Mg/(Mg + 0.9 * Fe_{total})atomic). *n.d.* not detected. GP277 and GP255→Olivine basalt (flow 1). GP252 and GP229→Three phenocryst basalt (flows 2 and 6 respectively). GP240→Ankaramite (flow 3). GP216 and GP61→basalt (flows 4 and 8 respectively). GP219, GP220→Hawaiite (flow 10). GP221, GP222 and GP224→Hawaiite (flows 9, 7 and 5 respectively). GP285, GP225 and GP239→Mugearite (dykes and sills). GP210→Ignimbrite (associated with flow 12). GP214→Rhyodacite (flow 12). GP235→Pitch Stone (associated with flow 12). GP291→Rhyolite (flow 11)

Petrogenesis

Effects of alteration

The concentrations of most elements in basalt and hawaiite samples display reasonable trends with some scatter on variation diagrams (Fig. 2). Mugearite samples exhibit more scatter possibly reflecting the occurrence of xenocrystic material in some samples. As a generalization Cu and Sr in basalt and hawaiite samples show the greatest amount of random behaviour on variation diagrams. These elements are notoriously mobile under zeolite facies conditions and may have suffered modification. The light REE (LREE) can also be affected by low temperature processes (*Condie* et al., 1977; *Hellman* et al., 1979) but essentially constant element ratios (e.g. La/Ce) indicate that they were immobile. In summary, for most elements, a reasonable assumption is that concentrations have not been substantially affected by alteration processes.

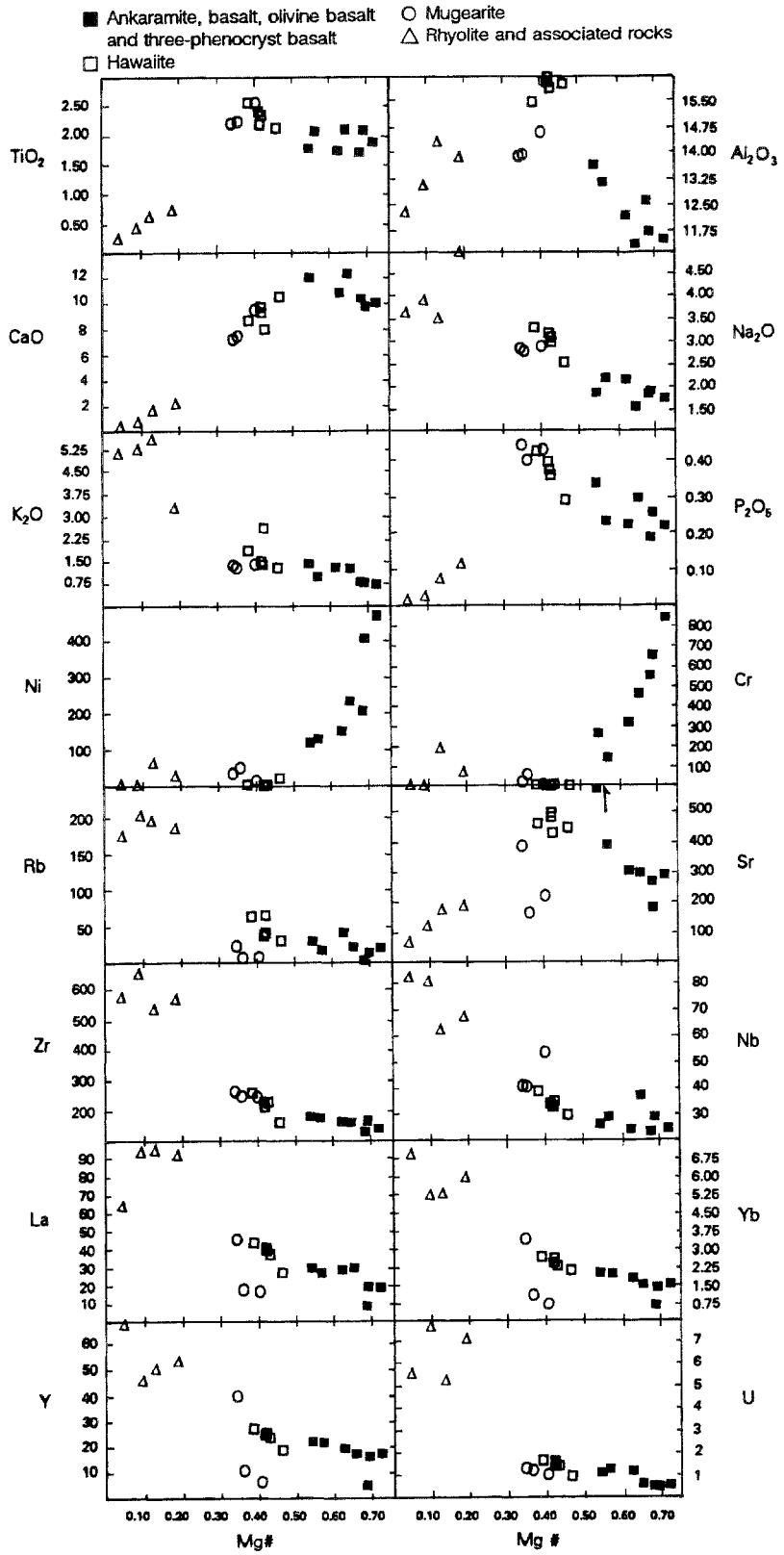
■ Ankaramite, basalt, olivine basalt and three-phenocryst basalt
□ Hawaiite
○ Mugearite
△ Rhyolite and associated rocks
TiO2
Al2O3
CaO
Na2O
K2O
P2O5
Ni
Cr
Rb
Sr
Zr
Nb
La
Yb
Y
U
Mg#
Mg #

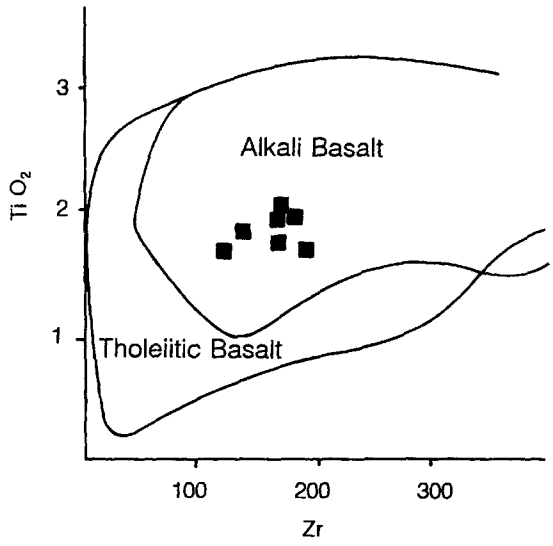

Fig. 3. Plot of Pavagadh basalts on the Zr (ppm) versus TiO_2 Oxide wt.%) diagram of *Floyd* and *Winchester* (1978)

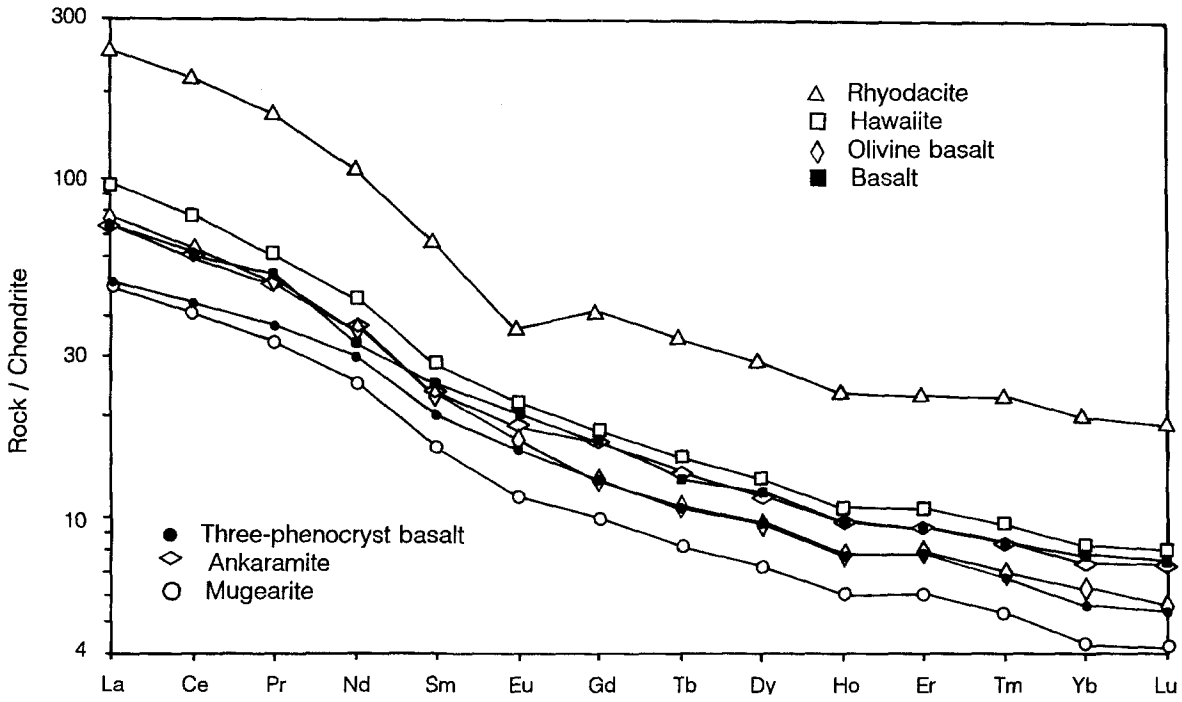

Fig. 4. Chondrite-normalized REE diagrams for representative Pavagadh rocks (three-phenocryst basalt, GP 252; olivine basalt, GP 277; ankaramite, GP 240; basalt, GP 216; mugearite, GP 225; hawaiite, GP 224; rhyodacite, GP 214). Normalizing values are from *Evenson* et al. (1978)

Fig. 2. Variation diagrams showing selected major element oxides (wt.%, volatile free) and trace elements (ppm) plotted against the differentiation index Mg# (where Mg# = Mg/(Mg+0.9*Fe_{total}) atomic). One point on the Sr diagram, indicated by the arrow plots off the graph. Samples plotting on the X axis of the Ni and Cr diagrams had concentrations at or below detection limits

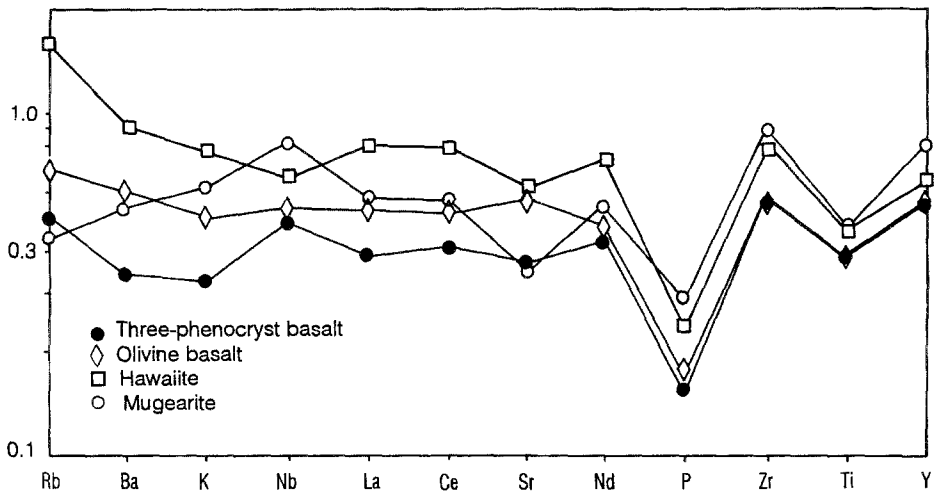

Fig. 5. Oceanic island basalt-normalized diagrams for average three-phenocryst basalt (GP 229 and GP 252), average olivine basalt, ankaramite and basalt (samples GP 255, GP 277, GP 240, GP 216, and GP 61), average hawaiite (samples GP 221, GP 224, GP 219, GP 220 and GP 222), and average mugearite (samples GP 285, GP 225 and GP 239). Normalizing values from *Fitton* et al. (1991) "mean by island"

Identification of primitive magma

Evidence from lherzolites suggests that mantle olivine has approximately a Fo_{90} composition (*Carswell*, 1980). Magmas formed in equilibrium with such olivine should have Mg# values between 0.70 and 0.72 (*Roeder* and *Emslie*, 1970; *Green*, 1971). Similarly, Ni concentrations in mantle olivine are approximately 3200 ppm and at magmatic temperatures, magma Ni/MgO ratios of 23–39 should be expected (Basaltic Volcanism Study Project, 1981, pp 421–426). The three-phenocryst basalt samples approximate these criteria (Mg# = 0.69–0.72; Ni/MgO = 32.2–34.6 respectively). In addition Cr concentrations (657 and 844 ppm respectively) are high. Apparently they are very primitive, if not "primary", basalts.

These are amongst the most primitive basalts reported from the Deccan basalt province. *Beane* and *Hooper* (1988) examined numerous occurrences of tholeiitic picrite basalts from the Western Ghats and concluded that no unfractionated lavas occur in the area. Extremely primitive basalts have been recovered from drill holes in the Dhandhuka-Wadhwan-Botad area, but, like the Pavagadh basalts, these appear "alkaline" and enriched in incompatible elements relative to most Deccan basalt magmas (*Krishnamurthy* and *Cox*, 1977; *Peng* and *Mahoney*, 1995). In petrologic provinces such as Hawaii tholeiitic magmas rarely if ever reach the surface undifferentiated but late alkaline magmas tend to be very primitive (*Clague* and *Dalrymple*, 1987). Moderately high Mg# values (~0.57) for the most-primitive Deccan basalts from the Rajpipla alkaline suite (*Krishnamurthy* and *Cox*, 1980) also support the idea that Deccan alkali basalts tend to be more primitive than tholeiitic basalts though these rocks are much more evolved than the most-primitive Pavagadh basalts.

Magma differentiation and evolution

More than one batch of magma must have been involved in generating the sequence of flows at Pavagadh because in some cases very primitive basalts (e.g. three-phenocryst basalt, flow 6) overlie highly evolved rocks (e.g. hawaiite, flow 5). However, the two most primitive flows (flow 2 and flow 6; samples GP252 and GP229, Table 3) are geochemically very similar but occur at different heights in the sequence suggesting that all rocks could have been generated from somewhat similar primary magmas. Low REE concentrations and scatter of mugearite data on the variation diagrams implies that these rocks are least likely to be genetically related to other rocks at Pavagadh Hill. The variation diagrams (Fig. 2) indicate a generalized magma differentiation scheme between primitive basalts and hawaiites as follows. Early removal of olivine and clinopyroxene accounts for decreasing MgO, Ni and Cr but concomitant increases in CaO and Al_2O_3 (Fig. 2; Table 3) imply that pyroxene and plagioclase fractionation were of less importance than olivine removal. Pyroxene probably became the dominant fractionating phase as basalts evolved into hawaiites beacuse CaO concentrations fall but Al_2O_3 continues to rise. TiO_2 concentrations rise slowly throughout the suite implying that Fe–Ti oxides were precipitated. Plagioclase may have been a more important fractionating phase in producing mugearite from hawaiite because Al_2O_3 and Sr concentrations fall (Fig. 2).

Mass balance (*Bryan* et al., 1969) and trace element modelling were used to test the above differentiation scheme. Production of hawaiites from primitive basalts was modelled in two stages based on changes in the trend lines of CaO and Al_2O_3 on variation diagrams (Fig. 2). Mugearite samples were not modelled because of their tendency to plot furthest from trend lines in Fig. 2. The two most primitive basalts (average of GP229 and GP252) were assumed parental to the two most evolved basalt samples (average of GP216 and GP61) which in turn were taken as parental to evolved hawaiite samples GP220 and GP222. Pavagadh mineral analyses supplemented by published Deccan mineral data were used in the mass balance calculations (Table 4). The results (Table 5) show a low R^2 value (sum of squared residuals) of 0.16 supporting generation of basalt from three-phenocryst basalt through removal of olivine, plagioclase, clinopyroxene and Fe-Ti oxides in proportions 55:27:12:6 with 65% of the original magma remaining. Approximation of the hawaiite composition was less successful ($R^2 = 0.82$) but suggests the removal of these minerals in proportions 8:13:77:2 with 74% of the basalt remaining. These results point to the importance of olivine and pyroxene fractionation during the evolution of Pavagadh alkali basalt just as recorded for other alkali basalts (e.g. Basaltic Volcanism Study Project, 1981, p 561). Similarly, *Krishnamurthy* and *Cox* (1977, 1980) concluded that plagioclase is an important phenocryst phase in the Deccan alkali basalts at Dhandhuka-Wadhwan-Botad and Rajpipla but due to its low density only small amounts of the mineral fractionated. Various workers have argued that plagioclase fractionation is important during the evolution of Deccan tholeiites (e.g. *Cox* and *Hawkesworth*, 1985; *Cox* and *Devey*, 1987; *Lightfoot* et al., 1990) though even in these rocks substantial plagioclase fractionation does not occur during the earliest stages of differentiation (rocks with MgO > 6.0 wt.%, *Sen*, 1986, 1987).

Table 4. *Mineral compositions used for modelling*

Oxide	Olivine-1	Olivine-2	Pyroxene	Plagioclase	Titano-magnetite
SiO_2	40.21	40.45	52.66	51.29	0.22
TiO_2	0.00	0.00	0.22	0.08	27.76
Al_2O_3	0.00	0.00	2.45	29.72	2.12
FeO	13.12	13.82	6.16	1.24	64.57
CaO	0.63	0.44	22.35	13.49	0.13
MgO	43.46	45.59	15.15	0.34	0.35
Na_2O	–	–	–	3.36	–
K_2O	–	–	–	0.22	–
MnO	0.65	0.50	0.00	–	–

Analysis in wt%. Total Fe as FeO. For parent three phenocryst basalt → model basalt, analysis in columns 1, 3, 4 and 5 were used for basalt → model hawaiite, analysis 2, 3, 4 and 5 were used. The analysis in column 4 plagioclase is from *Konda* (1985) and column 5 titanomagnetite is from *Krishnamurthy* and *Cox* (1977)

Trace element modelling was based on assumed Rayleigh fractionation (*Gast*, 1968), the mineral proportions and percentages of fractionation indicated from mass balance and partitioning coefficients given in Table 5. The poor correspondence between observed and predicted concentrations suggests that 1) the flows were not comagmatic or 2) the major element mass balance solution is not accurate or 3) processes other than crystal fractionation affected magma evolution. Of these, 1 may be the most important. Due to the eutectic melting behaviour of magmas, small changes in the percentage of melting will have a minor effect on major element concentrations (given equivalent source mineralogy and pressure) but a substantial impact on incompatible element concentrations at the low percentages of melting that generate alkaline magmas. Thus two magma batches could have similar major element compositions but very different Rb, Zr etc. concentrations. The possiblity that the discrepancies reflect crustal assimilation is explored below.

There is little evidence bearing on the nature and relationships of magma chambers that fed the flows. The presence of three phenocryst phases in the most primitive rocks indicates movement through long conduits, possibly dykes, prior to eruption at the surface (*Cox* and *Bell*, 1972; *Krishnamurthy* and *Cox*, 1977). As already pointed out the sequence of flows is not consistent with differentiation of a single parental magma; for example one of the most primitive flows occurs in the middle of the sequence. Thus it is possible that more than one magma chamber fed the flows.

Crustal contamination

Crustal assimilation is important in the evolution of many continental basaltic magmas (*De Paolo*, 1981; *Thompson* et al., 1982; *Dostal* and *Dupuy*, 1984; *Greenough* et al., 1989). Features commonly attributed to upper crustal assimilation include elevated Rb/Sr ratios (>0.12; *Krishnamurthy* and *Udas*,

Table 5. *Modelling results*

	Parent 3PB	Model Basalt	Basalt	Model Hawaiite	Hawaiite
Major elements (Wt%)					
SiO_2	47.85	50.63	50.79	50.85	50.33
TiO_2	1.99	2.07	1.90	2.35	2.50
Al_2O_3	11.70	13.48	13.56	16.30	16.10
FeO	11.61	11.06	11.17	12.32	12.13
MnO	0.17	0.07	0.17	0.20	0.17
MgO	13.79	6.97	6.97	4.01	4.05
CaO	10.07	11.90	11.94	9.39	9.34
Na_2O	1.82	2.32	2.05	2.62	3.27
K_2O	0.76	1.13	1.16	1.57	1.71
P_2O_5	0.24	0.37	0.29	0.40	0.41
Trace elements (ppm)					
Rb	15	23	22	30	52
Sr	283	364	680	852	475
Ba	176	261	380	508	486
Zr	153	235	176	237	244
Y	16	25	22	30	26
La	19	28	29	38	42
Eu	1.4	2.1	2.7	3.4	2.3
Yb	1.5	2.2	2.0	2.5	2.6
Cr	751	27	199	15	0
Ni	440	3	128	33	0
Modelling data					
Olivine		0.550		0.083	
Augite		0.120		0.769	
Plagioclase		0.268		0.132	
Fe-Ti Oxide		0.062		0.016	
% Crystallized		35		26	
R^2		0.16		0.82	

Major element oxides are given in wt.% normalized to 100% volatile free. Total Fe as FeO. a) Parent 3PB is the average of three-phenocryst basalt samples GP229 and GP252. Model Basalt is the modelled composition of basalt given in the third column. Basalt in column three is an average of samples GP216 and GP61. Model Hawaiite is the attempt to reproduce the Hawaiite composition in the last column (an average of analyses GP220 and GP222) assuming Basalt (column three) as parent. b) Major elements modelled using mass balance calculations of *Bryan* et al. (1969). Proportions of minerals removed are given under modelling data. Mineral compositions used in the calculations are given in Table 4. c) Trace elements were modelled using the Rayleigh fractionation equation (*Gast*, 1968) with phase proportions and % crystallization as indicated from the mass balance calculations. Partitioning coefficients used for Rb, Sr, Ba, Zr, Y, La, Eu, Yb, Cr, and Ni are in plagioclase: 0.08, 1.50, 0.30, 0.02, 0.02, 0.02, 0.15, 0.34, 0.05, 0.01, and 0.04; in olivine: 0.0, 0.01, 0.01, 0.01, 0.01, 0.01, 0.02, 0.04, 2, 7, and 20.0; in augite: 0.0, 0.08, 0.0, 0.01, 0.01, 0.08, 0.35, 0.40, 10.0, and 4.5; and in Fe-Ti oxide: 0.0, 0.0, 0.0, 0.0, 0.14, 0.10, 0.10, 0.17, 97.0, 23.0. Partitioning coefficients are from *Evans* (1978), *Frey* et al. (1974) and *Philpotts* and *Schnetzler* (1970). d) Rows labelled olivine, augite etc. give the fractions of each phase removed during modelling. % Crystallized gives the percentage of the magma removed as crystals. R^2 is the sum of squared residuals and indicates how well the modelled composition matches the observed composition

1981), positive peaks for K and negative Nb anomalies on element normalized diagrams (*Dostal* and *Dupuy*, 1984) and Th/Nb ratios in excess of those in MORB (>0.2, *Kempton* et al., 1991). Average Pavagadh geochemical patterns (Fig. 5) illustrate that not even the highly evolved rocks (e.g. hawaiites and mugearites) display K and Nb anomalies. In general Rb/Sr and Th/Nb ratios give no indication of crustal assimilation.

Numerous isotopic studies (Nd, Sr, Pb and O) show that Deccan tholeiites experienced varying degrees of crustal contamination ranging from minimal (Ambenali Formation) to large (Bushe Formation; e.g. *Cox* and *Hawkesworth*, 1985; *Devey* and *Cox*, 1987; *Lightfoot* and *Hawkesworth*, 1988; *Lightfoot* et al., 1990). Contamination was apparently from various crustal sources including lower crustal amphibolites for lower formations of the Western Deccan traps (Jawhar through Khandala; *Peng* et al., 1994). Trace element data are not as useful for detecting the effects of crustal contamination as are isotopic data. However, Pavagadh basalts show Th/Nb ratios (for example) as low or lower than those observed in the Deccan province. Thus, on the basis of trace element data they are amongst the least affected by crustal contamination. *Devey* and *Cox* (1987) found that primitive Poladpur Formation tholeiites tend to be more contaminated in terms of Sr isotopic ratios than more evolved basalts. Primitive Pavagadh basalts show no more evidence for contamination than more evolved basalts.

Genesis of rhyolites and associated rocks

At least three hypotheses may explain the origin of rhyolites in flood basalt provinces: 1) they represent the end products of magmatic differentiation, 2) they form through sialic contamination of basalt (e.g. *Alexander*, 1980) or 3) they represent independent magmas with no genetic link to the basalts (*Bose*, 1972; *Sukheswala*, 1981). Geochemical variation diagrams (Fig. 2) and SiO_2 contents (Table 2) show a compositional gap between Pavagadh rhyolites/rhyodacites and more mafic rocks suggesting that the two are not genetically related. Where rhyolites occur in flood basalt provinces, including the Deccan (*Krishnamurthy* and *Cox*, 1980), compositional gaps are common. The rhyolites generally occur at the top of the volcanic sequence. As at Pavagadh, Deccan rhyolites reported from Rajpipla are associated with alkaline mafic rocks. Rhyolites are rare in the Deccan province and they tend to occur along zones of crustal weakness (*Krishnamurthy* and *Cox*, 1980). Together, these observations imply that the zones of weakness extend into the mantle facilitate the exit of magmas of deeper (alkaline) origin and encourage crustal pooling of magma. The heat of crystallization eventually melts the crust producing late-stage silicic magmas chemically unrelated, or distantly related, to the basalts.

Basaltic magma generation

Zr-TiO_2 diagram (Fig. 3), Nb/Y ratios greater than 1 (*Pearce* and *Cann*, 1973) and the modestly steep slopes on chondrite-normalized REE diagrams, suggest that these are mildly alkaline rocks. The occurrence and association of mugearites and hawaiites with alkali basalts is well established (Basaltic Volcanism Study Project,

p 168). Melting experiments on lherozolites indicate that alkaline magmas are generated by small percentages of melting (< 20% melting) compared to tholeiites (20–30%), which are produced at lower pressures (< 15–20 kb; e.g. *Jaques* and *Green*, 1980; *Takahashi* and *Kushiro*, 1983). Similarly, trace element modelling experiments suggest that alkaline magmas represent comparatively small percentages of melting (e.g. *Gast*, 1968; *Frey* et al., 1978). Major-element-based equations developed by *Chen* (1988) return percentages of melting between 7 and 10% for the most primitive rocks from Pavagadh. Chondrite-normalized heavy REE concentrations (Yb_{cn} and Lu_{cn}) in the most primitive Pavagadh basalts are about 6 indicating that the basalts were generated at relatively high pressures within the stability field of garnet (*Kay* and *Gast*, 1973).

Despite being alkaline these rocks are not nearly so incompatible-enriched as Deccan basalts from the Rajpipla alkalic suite. For example typical Rb, Ba, Zr and La concentrations in Rajpipla ankaramitic basalts (Mg# = 0.57) are 72, 1100, 290 and 65 ppm (*Krishnamurthy* and *Cox*, 1980) compared with 15, 290, 170 and 28 ppm in Pavagadh basalt GP 216 (Table 3, Mg# = 0.56). Absolute concentrations in tholeiitic basalts are still lower. For example Poladpur or Ambenali Formation tholeiites with Mg#~0.55 typically have <10 ppm Rb, 80–90 ppm Ba, 140–150 ppm Zr and 10–12 ppm La based on data from *Lightfoot* et al. (1990). The higher absolute incompatible element concentrations of alkali basalts have long been attributed to lower percentages of mantle melting and greater pre- or syn-melting source region metasomatic enrichment (e.g. *Sun* and *Hanson*, 1975; *Cullers* et al., 1985).

Melting of subcontinental lithospheric mantle, metasomatically enriched by pre-basalt subduction processes, imparts a different pattern of trace element enrichment on basalts than that imposed by asthenospheric processes (*Fitton* et al., 1988, 1991; *Kempton* et al., 1991). Trace element characteristics inherited from the mantle lithosphere include Ba enrichment and depletions in Nb and Ti compared to oceanic island basalts (OIB). These characteristics reflect earlier involvement of the lithosphere in subduction processes wherein slab-derived metasomatising fluids enrich the lithospheric mantle in large ion lithophile elements (especially Ba) and high field-strength elements (e.g., *Macdonald* et al., 1985; *Mauger*, 1988; *Wyman* and *Kerrich*, 1989). Either the fluids cannot carry Ti and Nb or they result in stabilization of oxide phases that retain Ti and Nb during subsequent melting events. Averaged data for the Pavagadh alkali basalts show a *positive* Nb anomaly, no Ba anomaly and a slight negative Ti anomaly that support an asthenospheric origin (Fig. 5).

Figure 6 compares Pavagadh alkali basalts with other Deccan basalts, Cenozoic continental mafic rocks from the Western Great Basin, U.S.A., bearing a subcontinental lithospheric mantle imprint, and OIB. In Fig. 6a La/Y ratios give a measure of source region enrichment/percentage of melting with high values indicating more alkaline magmas. High Zr/Nb and La/Nb ratios and low La/Ba ratios indicate involvement of the subcontinental lithospheric mantle in magma genesis (Fig. 6a, b) or a role for crustal assimilation in magma evolution. In order to minimize the influence of crustal assimilation only rocks with Mg# values greater than 0.50 were plotted. A higher cut-off value would have been used except that few Deccan tholeiites would meet the plotting criteria.

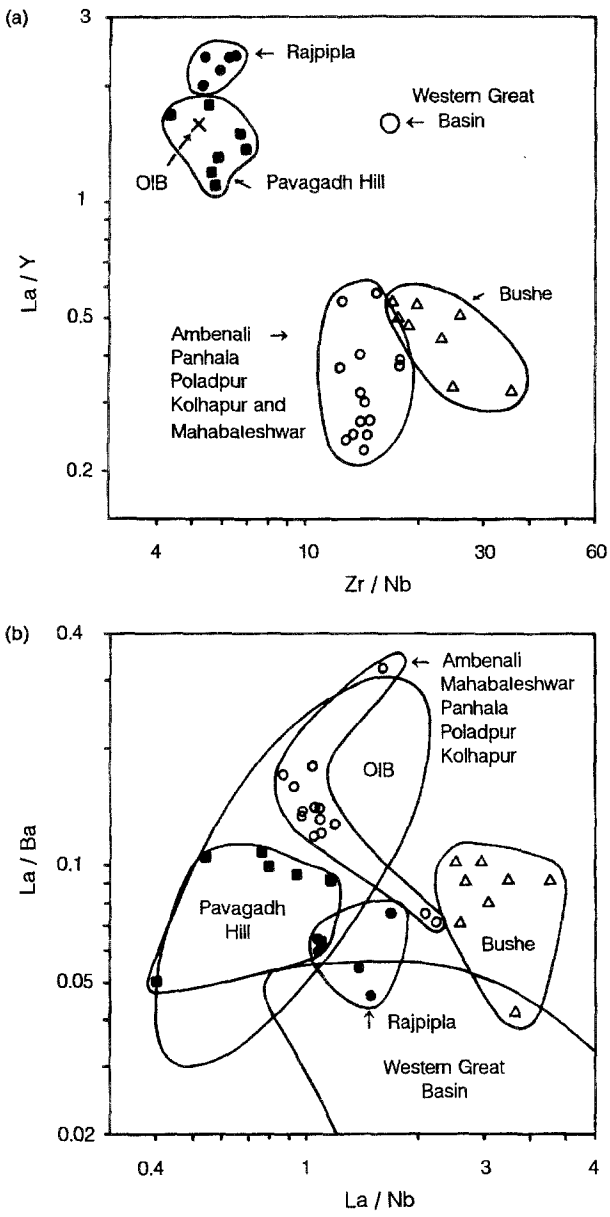

Fig. 6. Plots of **a** La/Y versus Zr/Nb and **b** La/Ba versus La/Nb. Open symbols are Deccan tholeiites and closed symbols Deccan alkali basalts. All data have Mg# values greater than 0.50. Averages in (**a**) and fields in (**b**) are for Western Great Basin, U.S.A., basalts and Oceanic Island Basalts (OIB; *Fitton* et al., 1991). Sources: Rajpipla alkali basalts, *Krishnamurthy* and *Cox* (1980); tholeiitic data, *Cox* and *Hawkesworth* (1985), *Lightfoot* and *Hawkesworth* (1988) and *Lightfoot* et al. (1990). See text for discussion

The Pavagadh Hill alkaline rocks have OIB-like Zr/Nb, La/Nb and La/Ba ratios suggesting an asthenospheric origin and providing no evidence for a lithospheric mantle component or upper crustal assimilation. If subcontinental lithosphere was involved in the formation of Pavagadh basalts it was chemically similar to asthenospheric mantle generating basalts at oceanic islands.

The Rajpipla alkaline rocks have slightly higher La/Nb ratios that skirt the OIB field supporting a small lithospheric mantle component in their petrogenesis. Deccan tholeiitic basalts from the Ambenali, Panhala, Poladpur, Kolhapur and Mahabaleswar Formations mostly plot within the OIB field (Fig. 6b). High Zr/Nb ratios equivalent to those in Western Great Basin, U.S.A., mafic rocks should not

be construed as evidence for a significant lithospheric component in their origin because Nb is much more incompatible than Zr thus Zr/Nb ratios tend to be higher in tholeiites than in alkali basalts (*Sun* and *McDonough*, 1989). Deccan tholeiites from the Bushe Formation have high La/Nb and Zr/Nb ratios accompanied by high Th/Nb ratios (0.6–1.3) reflecting upper crustal assimilation.

Combined trace element and isotopic studies of Deccan tholeiites have succeeded in identifying a lithospheric mantle imprint particularly in some Deccan Mahabaleswar Formation tholeiites (*Lightfoot* and *Hawkesworth*, 1988; *Lightfoot* et al., 1990). Alkali basalts from the Dhandhuka-Wadhwan-Botad drill holes and in Madagascar (adjacent to the drill hole sites prior to Cretaceous rifting) exhibit a mantle lithosphere signature (*Mahoney* et al., 1991; *Peng* and *Mahoney*, 1995). However, comparison with other flood basalt sequences (e.g. Karoo and Parana) shows that the extent of the subcontinental mantle lithospheric imprint and frequency with which it is expressed are much lower in the Deccan flood basalt province (*Lightfoot* and *Hawkesworth*, 1988). Apparently most geochemical data support a largely asthenospheric origin for the majority of Deccan flood basalts. The relatively young age (late formation) of the Pavagadh Hill rocks compared to the bulk of Deccan volcanism indicates that if the mantle lithosphere was going to be involved in the melting process as a result of plume impingement then these are the rocks to show such a relationship.

Fitton et al. (1991) point out that it is not clear why mafic magmas from some provinces show a strong lithospheric imprint whereas those from other continental areas largely lack these features. One possibility they suggest is that areas showing the imprint overlie plumes which are sufficiently hot, that the lithosphere is softened and becomes involved in melting processes. There are problems with this in the Deccan province. The volume and composition of mafic magma produced through lithospheric extension and mantle decompression can be estimated (*McKenzie* and *Bickle*, 1988). These numerical models indicate that the volume of magma produced by decompression is highly dependent on the potential temperature of the mantle (the temperature the mantle would have if brought to the surface adiabatically). A potential temperature increase of 150° above normal results in a three-fold increase in the volume of melt produced. The Deccan flood basalt province is at least moderately large (*White*, 1989), implying that the plume had a high potential temperature. If "hot" plumes involve the mantle lithosphere in magma production then surely Deccan magmas should show a strong lithosphere imprint.

Lightfoot and *Hawkesworth* (1988) proposed that the reason few Deccan basalt flows bear the lithospheric imprint is that the Deccan was largely erupted at the margin of, rather than within, a continent. Another possibility is that time plays an important role in determining whether the mantle lithosphere gets involved in melting. Areas experiencing long-lived extension and igneous activity may provide the time required to heat the lithosphere and involve it in melt production. Most Deccan igneous activity occurred over a very short time span (1–0.5 Ma; *Duncan* and *Pyle*, 1988; *White*, 1989) whereas basalt production in the western United States, where many magmas display the lithospheric imprint spans more than 25 million years (*Fitton* et al., 1991). It may also be significant that subduction preceded the production of flood basalts in western North America (*Lipman* et al.,

1972) such that magmas produced during the earlier igneous activity could have preheated the lithosphere. Prior to the Deccan event the Indian-African continent was tectonically inactive.

Acknowledgements

K. R. H. is thankful to Dr. *G. Sen*, Florida International University, Miami who provided electron microprobe analyses of minerals. Ms. *H. Muggeridge* did the drafting and Ms. *D. Sarnecki* and *C. Neid* prepared the tables. *K. G. Cox* provided a very helpful review. Funding for *JDG* came from the Natural Sciences and Engineering Research Council of Canada. *A.C.C.* extends his gratitude to the University Grants Commission of India for financial support of the project.

References

Alexander PO (1980) The Pavagarh rhyolites. J Geol Soc India 21: 453–457

Alexander PO (1981) Age and duration of Deccan volcanism: K-Ar evidence. In: *Subba Rao KV, Sukheswala RN* (eds) Deccan volcanism and related basalt provinces in other parts of the world. Geological Society of India, Memoir No 3, pp 244–259

Basaltic Volcanism Study Project (1981) Basaltic volcanism on the terrestrial planets. Pergamon Press, New York, 1286 pp

Basu AR, Renne PR, DasGupta DK, Teichmann F, Poreda RJ (1993) Early and late alkali igneous pulses and a high-^{3}He plume origin for the deccan flood basalts. Science 261: 902–906

Bean JE, Hooper PR (1988) A note on the picrite basalts of the Western Ghats, Deccan traps, India. In: *Subbaro KV* (ed) Deccan flood basalts. Geological Society of India, Memoir 10, pp 117–133

Bryan WB, Finger LW, Chayes F (1969) Estimating proportions in petrographic mixing equations by least-squares approximation. Science 163: 926–927

Bose MK (1972) Deccan basalts. Lithos 5: 131–145

Carswell DA (1980) Mantle derived lherzolite nodules associated with kimberlite, carbonatite and basalt magmatism: a review. Lithos 13: 121–138

Chatterjee SC (1961) Petrology of Pavagarh Hill, Gujarat. J Geol Soc India 2: 61–67

Chen C-H (1988) Estimation of the degree of partial melting by (Na_2O+K_2O) and (Al_2O_3/SiO_2) of basic magmas. Chem Geol 71: 355–364

Clague DA, Dalrymple GB (1987) The Hawaiian-Emperor volcanic chain, part 1. Geologic evolution. In: *Decker RW, Wright TL, Stauffer PH* (eds) Volcanism in Hawaii, vol 1. U.S. Geological Survey Professional Paper 1350, pp 5–54

Condie KC, Viljoen MJ, Kable EDI (1977) Effects of alteration on element distribution in Archean tholeiites from Barberton Greenstone Belt, South Africa. Contrib Mineral Petrol 64: 75–89

Cox KG, Bell JD (1982) A crystal fractionation model for the basaltic rocks of the New Georgia Group, British Solomon Islands. Contrib Mineral Petrol 37: 1–13

Cox KG, Hawkesworth CJ (1985) Geochemical stratigraphy of the Deccan traps at Mahabaleshwar, Western Ghats, India, with implications for open system magmatic processes. J Petrol 26: 355–377

Cox KG, Devey CW (1987) Fractionation processes in Deccan traps magmas: comments on the paper by G. Sen – Mineralogy and petrogenesis of the Deccan trap lava flows around Mahabaleshwar, India. J Petrol 28: 235–238

Cullers RL, Ramakrishnan S, Berendsen P, Griffin T (1985) Geochemistry and petrogenesis of lamproites, Late Cretaceous age, Woodson Country, Kansas, U.S.A. Geochim Cosmochim Acta 49: 1383–1402

De Paolo DJ (1981) Trace element and isotopic effects of combined wallrock assimilation and fractional crystallisation. Earth Planet Sci Lett 53: 189–202

Devey CW, Cox KG (1987) Relationships between crustal contamination and crystallisation in continental flood basalt magmas with special reference to the Deccan Traps of the Western Ghats, India. Earth Planet Sci Lett 84: 59–68

Dostal JB, Dupuy C (1984) Geochemistry of the North Mountain Basalts (Nova Scotia, Canada). Chem Geol 45: 245–261

Duncan RA, Pyle DG (1988) Rapid eruption of the Deccan flood basalts, Western India. In: *Subbaro KV* (ed) Deccan flood basalts. Geological Society India, Memoir 10, pp 1–9

Evans JL (1978) An alkalic volcanic suite of the Labrador Trough, Labrador. Thesis, Memorial University of Newfoundland, St. John's, Newfoundland, Canada

Evensen NM, Hamilton PJ, O'Nions RK (1978) Rare-earth abundances in chondritic meteorites. Geochim Cosmochim Acta 42: 1199–1212

Fitton JG, James D, Kempton PD, Ormerod DS, Leeman WP (1988) The role of lithospheric mantle in the generation of late Cenozoic basic magmas in the Western United States. J Petrol [Special Lithosphere Issue]: 331–349

Fitton JG, James D, Leeman WP (1991) Basic magmatism associated with Late Cenozoic extension in the Western United States: compositional variations in space and time. J Geophys Res 96: 13693–13711

Floyd PA, Winchester JA (1978) Indentification and discrimination of altered and metamorphosed volcanic rocks using immobile elements. Chem Geol 21: 291–306

Frey FA, Bryan WB, Thompson G (1974) Atlantic ocean floor: geochemistry and petrology of basalts from Legs 2 and 3 of the Deep Sea Drilling Project. J Geophys Res 79: 5507–5527

Frey FA, Green DH, Roy SD (1978) Integrated models of basalt petrogenesis: a study of quartz tholeiites to olivine melilitites from southeastern Australia utilizing geochemical and experimental petrological data. J Petrol 19: 463–513

Gast PW (1968) Trace-element fractionation and the origin of tholeiitic and alkaline magma types. Geochim Cosmochim Acta 32: 1057–1086

Green DH (1971) Composition of basaltic magmas as indicators of conditions of origin: application to oceanic volcanism. Phil Transact Roy Soc Lond A268: 707–725

Greenough JD, Jones LM, Mossman D (1989) The Sr isotopic composition of early Jurassic mafic rocks of Atlantic Canada: implications for assimilation and injection mechanisms affecting mafic dykes. Chem Geol [Isotope Geoscience Sect] 80: 17–26

Hari KR (1991) Mineralogical and fluid inclusion studies of primary constituents of mafic and ultramafic rocks of Pavagadh Hill (Deccan Traps), Gujarat. Thesis, Vikram University, Ujjain, India, 110 p

Hari KR, Santosh M, Chatterjee AC (1991) Primary silicate melt inclusions in olivine phenocrysts from Pavagadh igneous suite, Gujarat. J Geol Soc India 37: 343–350

Hellman PL, Smith RE, Henderson P (1979) The mobility of the rare earth elements: evidence and implications from selected terrains affected by burial metamorphism. Contrib Mineral Petrol 71: 23–44

Jaques AL, Green DH (1980) Anhydrous melting of peridotite at 0–15 kb and the genesis of tholeiitic basalts. Contrib Mineral Petrol 73: 287–310

Kay RW, Gast PW (1973) The rare earth content and origin of alkali-rich basalts. J Geol 81: 653–682

Kempton PD, Fitton JG, Hawkesworth CJ, Ormerod DS (1991) Isotopic and trace element constraints on the composition and evolution of the lithosphere beneath the Southwestern United States. J Geophys Res 96: 13713–13735

Krishnamurthy P, Cox KG (1977) Picrite basalts and related lavas from the Deccan traps of Western India. Contrib Mineral Petrol 62: 53–75

Krisnamurthy P, Cox KG (1980) A potassium-rich alkalic suite from the Deccan Traps, Rajpipla, India. Contrib Mineral Petrol 73: 179–189

Krishnamurthy P, Udas GR (1981) Regional geochemical characters of the Deccan trap lavas and their genetic implications. Geological Society of India, Memoir No 3, pp 394–418

Krishnan MS (1982) Geology of India and Burma 6th ed. CBS Publishers, Delhi, 536 p

Lightfoot P, Hawkesworth C (1988) Origin of Deccan trap lavas: evidence from combined trace element and Sr-, Nd- and Pb-isotope studies. Earth Planet Sci Lett 91: 89–104

Lightfoot PC, Hawkesworth CJ, Devey CW, Rogers NW, Van Calsteren PWC (1990) Source and differentiation of Deccan trap lavas: implications of geochemical and mineral chemical variations. J Petrol 31: 1165–1200

Lipman PW, Prostka HJ, Christiansen RL (1972) Cenozoic volcanism and plate-tectonic evolution of the Western United States, I. Early and Middle Cenozoic. Phil Transact Roy Soc Lond (Series A) 271: 217–248

Longerich HP, Jenner GA, Fryer BJ, Jackson SE (1990) Inductively coupled plasma-mass spectrometric analysis of geologic samples: a critical evaluation based on case studies. Chem Geol 83: 105–118

Macdonald R., Thorpe RS, Gaskarth JW, Grindrod AR (1985) Multi-component origin of Caledonian lamprophyres of northern England. Mineral Mag 49: 485–494

Mohoney J, Nicollet C, Dupuy C (1991) Madagascar basalts: tracking oceanic and continental sources. Earth Planet Sci Lett 104: 350–363

Mauger RL (1988) Geochemical evidence for sediment recycling from North Carolina (U.S.A.) minettes. Can Mineral 26: 133–141

McKenzie D, Bickle MJ (1988) The volume and composition of melt generated by extension of the lithosphere. J Petrol 29: 526–679

Pearce JA, Cann JR (1973) Tectonic setting of basic volcanic rocks determined using trace element analyses. Earth Planet Sci Lett 19: 290–300

Peng ZX, Mahoney JJ (1995) Drillhole lavas from the northwestern Deccan Traps, and the evolution of Réunion hotspot mantle. Earth Planet Sci Lett 134: 169–185

Peng ZX, Mahoney JJ, Hooper P, Harris C, Beane J (1994) A role for lower continental crust in flood basalt genesis? Isotopic and incompatible element study of the lower six formations of the western Deccan Traps. Geochim Cosmochim Acta 58: 267–288

Philpotts JA, Schnetzler CC (1970) Phenocryst-matrix partitioning coefficients for K, Rb, Sr and Ba with applications to anorthosite and basalt genesis. Geochim Cosmochim Acta 34: 307–322

Roeder PL, Emslie RF (1970) Olivine-liquid equilibrium. Contrib Mineral Petrol 59: 275–289

Sen G (1986) Mineralogy and petrogenesis of the Deccan trap lava flows around Mahabaleshwar, India. J Petrol 27: 627–663

Sen G (1987) Reply to Cox and Devey. J Petrol 28: 239–240

Sinha RC, Tiwari BD (1964) Geochemistry of the volcanic rocks of Pavagadh. Proceedings, 22nd International Geological Congress, New Delhi, Section 7, pp 104–125

Sukheswala RN (1981) Deccan basalt volcanism. Geological Society of India, Memoir No 3, pp 8–18

Sun SS, Hanson GN (1975) Origin of Ross Island basanitoids and limitations upon the heterogeneity of mantle sources for alkali basalts and nephelinites. Contrib Mineral Petrol 52: 77–106

Sun S-s, McDonough WF (1989) Chemical and isotopic systematics of oceanic basalts: implications for mantle composition and processes. In: *Saundars AD, Norry MJ* (eds) Magmatism in the ocean basins. Geological Society Special Publication No 42, pp 313–345

Takahashi E, Kushiro I (1983) Melting of dry peridotite at high pressures and basalt magma genesis. Am Mineral 68: 659–679

Thompson RN, Dickin AP, Gibson IL, Morrison MA (1982) Elemental fingerprints of isotopic contamination of Hebridean Palaeocene mantle-derived magmas by Archean sial. Contrib Mineral Petrol 79: 159–168

Tiwari BD (1971) Magmatic differentiation of volcanic rocks of Pavagadh Gujarat, India. Bull Volcanol 35: 1129–1177

White RS (1989) Igneous outbursts and mass extinctions. Eos 70: 1480–1491

Wyman DA, Kerrich R (1989) Archean lamprophyre dikes of the Superior Province, Canada: distribution, petrology and geochemical characteristics. J Geophys Res 94: 4667–4696

Authors' addresses: *J. D. Greenough*, Department of Earth and Ocean Sciences, University of British Columbia, Okanagan University College, Kelowna, B.C., Canada, V1V 1V7; *K. R. Hari*, Department of Geology, Government Arts and Science College, Durg (M.P.), India, 491001; *A. C. Chatterjee*, School of Studies in Geology, Vikram University, Ujjain (M.P.) India; *M. Santosh*, Centre for Earth Science Studies, P.B. 7250, Akkulam, Trivandrum 695031, India.